Minimum-error discrimination of entangled quantum states

Y. Lu,[1] N. Coish,[1] R. Kaltenbaek,[1] D.R. Hamel,[1] S. Croke,[1,2] and K.J. Resch[1,*]

[1] *Institute for Quantum Computing and Department of Physics & Astronomy, University of Waterloo, Waterloo, Canada, N2L 3G1*

[2] *Perimeter Institute for Theoretical Physics, Waterloo, Canada, N2L 2Y5*

Strategies to optimally discriminate between quantum states are critical in quantum technologies. We present an experimental demonstration of minimum error discrimination between entangled states, encoded in the polarization of pairs of photons. Although the optimal measurement involves projecting onto entangled states, we use a result of Walgate *et al.* to design an optical implementation employing only local polarization measurements and feed-forward, which performs at the Helstrom bound. Our scheme can achieve perfect discrimination of orthogonal states and minimum error discrimination of non-orthogonal states. Our experimental results show a definite advantage over schemes not using feed-forward.

The ability, or inability, to perfectly distinguish between different quantum states is a defining feature of quantum mechanics and the basis of many quantum technologies. A typical scenario is that one wants to distinguish between one of two possible quantum states. If the two states are orthogonal, then there exists a measurement that can always distinguish between them with certainty. While there is no such test for non-orthogonal states, there are many ways to quantify how well a measurement distinguishes between them, and each defines a different strategy [1–11]. The most commonly considered are the minimum error [3–5] and unambiguous discrimination strategies [6–8]; the former arises naturally as an extension of classical hypothesis testing to the quantum realm while the latter is a peculiarly quantum strategy where error-free discrimination may sometimes be achieved by allowing for the possibility of an inconclusive outcome.

Each strategy is defined by optimizing a specific figure of merit over all possible measurements. However, whether the optimal measurement is achievable in practice depends on the physical system in question and its practical limitations. Experimental demonstrations of quantum state discrimination protocols to date have all used either the polarization or the spatial paths of light to encode the quantum information. Thus far, measurements consist of linear optics and photodetectors to measure the intensity of light in different paths; as the proportion of light reaching any given detector is the same for a beam of single photons and a weak classical source, almost all used attenuated lasers. The optimal minimum error [12, 13], unambiguous [14–16], maximum mutual information [12, 13, 17], and maximum confidence [18] strategies were implemented in this way. A very recent work investigated a state discrimination strategy using heralded single photons from down-conversion [19].

Here, we experimentally demonstrate state discrimination between pairs of *entangled* states, a truly quantum regime. We separately consider discrimination of orthogonal and non-orthogonal states. For the orthogonal case, one can always perform a projective measurement onto the states themselves to achieve perfect discrimination. In the non-orthogonal case, the theory describing the optimal measurements for single qubits [1–11] may readily be applied to pairs of entangled states. However, experimental constraints may prohibit implementing these optimal measurements. Specifically, with optical polarization high-fidelity local polarization measurements are possible, but entangling measurements are very difficult [20]. One might expect these constraints to limit our ability to discriminate between entangled states, but this is not the case. *Any* two orthogonal pure states, irrespective of their entanglement or multipartite structure, may be perfectly discriminated using only local operations and classical communication (LOCC) [22]. Further, any two non-orthogonal pure states can be optimally discriminated by LOCC, according to both the minimum error [23] and unambiguous discrimination [24–26] figures of merit. This highlights how to overcome seeming limitations of a physical system by using its resources more effectively. Conversely, and equally surprisingly, there exist sets of orthogonal *product* states between which per-

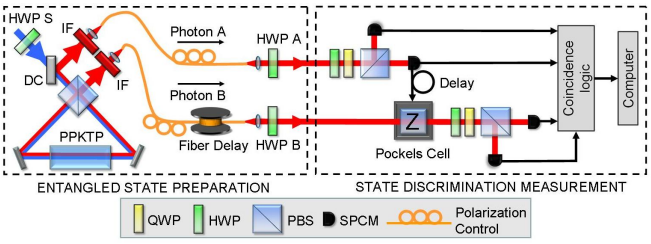

FIG. 1: Experimental setup. Half-wave plates S, A, and B were rotated to prepare polarization entangled states from the source. Feed-forward was achieved using a fast Pockels cell (PC) which performs the identity when off, or a phase flip (Pauli-Z) when on. We detect photons at single-photon counting modules (SPCM) and monitor coincidence events. With the PC off we also used this setup for quantum state tomography. Quarter-wave plate (QWP); polarizing beamsplitter (PBS); periodically-poled KTP crystal (PPKTP); interference filter (IF). See text for more details.

fect discrimination is *not* possible by LOCC [21]. The relationship between entanglement and LOCC discrimination is not simple, but helps shed some light on the power and limitations of LOCC.

The key insight for discriminating pairs of entangled states via LOCC was developed by Walgate *et al.* [22]. They showed that any two orthogonal quantum states, $|\phi\rangle$ and $|\psi\rangle$, where Alice has subsystem A and Bob has subsystem B, can be written in the form, $|\phi\rangle = \sum_i c_i|i\rangle_A|\eta_i\rangle_B$ and $|\psi\rangle = \sum_i d_i|i\rangle_A|\eta_i^\perp\rangle_B$, where $\{|i\rangle\}$ is a basis for subsystem A and $\langle\eta_i|\eta_i^\perp\rangle = 0$. Note that $\langle i|j\rangle = \delta_{ij}$ but $|\eta_i\rangle$ and $|\eta_j\rangle$ need not be orthogonal, differentiating this decomposition from the more widely known Schmidt decomposition. By viewing the states in this way, a strategy for distinguishing them becomes clear. Alice measures in the basis $\{|i\rangle\}$ and sends her result to Bob. Bob then orients his measurement device to distinguish between $|\eta_i\rangle$ and $|\eta_i^\perp\rangle$. In general, Bob needs to be able to change his measurement basis based on Alice's measurement outcome; this is called *feed-forward*. For two non-orthogonal pure states, the minimum-error, or Helstrom [3], measurement for discriminating between them is a projective measurement, i.e., there must be two orthogonal states that are perfectly discriminated by this measurement. Since such a measurement can be performed by LOCC, the minimum-error measurement to discriminate between any pair of non-orthogonal pure states may also be performed using LOCC [23]. For pure states with more than two subsystems, one can use LOCC for optimal discrimination by employing this strategy iteratively [22].

To implement this protocol experimentally, we constructed the setup shown in Fig. 1. A 404.5 nm, 0.25 mW grating-stabilized diode laser pumps a polarization-based Sagnac interferometer, producing 809-nm polarization-entangled photon pairs via type-II parametric down-conversion in a 25-mm long periodically-poled KTP (PPKTP) crystal [27–29]. The down-converted photons are coupled into single-mode fibres. When these fibres are directly connected to our single-photon counting detectors (Perkin Elmer SPCM-AQ4C) we typically measure coincidence rates of 7 kHz and singles rates of 60 kHz. Using the half-wave plate in the source (HWP S) we control the degree of polarization entanglement of the photon pairs. When set to produce maximum entanglement, we typically measure a fidelity [30], $F = 0.97$, with the target Bell state, and tangle [31], $\tau = 0.93$. The polarization of the photons is measured using analyzers consisting of a HWP, a quarter-wave plate (QWP), and a polarizing beam-splitter (PBS). Signals detected in the transmitted arm of the PBS in the analyzer for photon 1 are delayed by 250ns and then trigger a Pockels cell (Leysop RTP4-20-AR800) that implements a Pauli-Z operation, Z, ($|\mathbf{H}\rangle \to |\mathbf{H}\rangle$, $|\mathbf{V}\rangle \to -|\mathbf{V}\rangle$) on photon 2.

In the first part of our experiment, we investigate a set

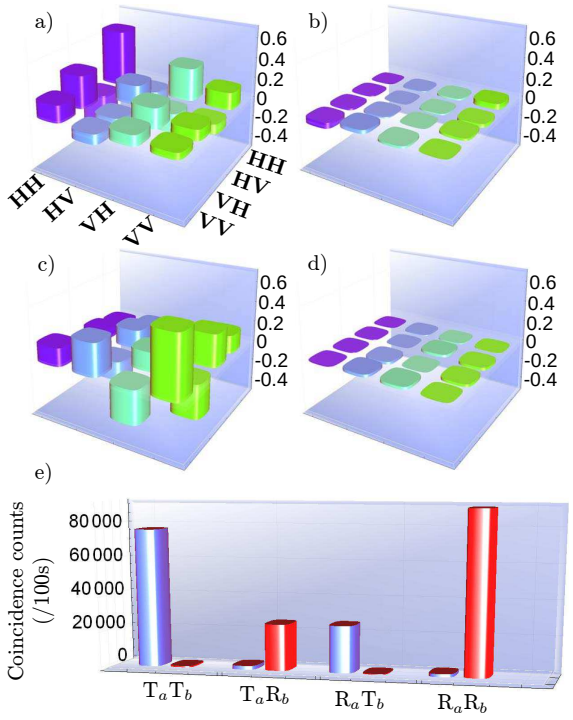

FIG. 2: Discrimination of two orthogonal entangled states. We set HWPs S, A, and B to prepare the state $|\phi_0\,(30^\circ)\rangle$ and used quantum state tomography to measure the state produced. The density matrix is depicted as a bar chart in a) real part and b) imaginary part. The fidelity with the target state is 0.981 ± 0.002. Similarly, we prepared $|\phi_1\,(60^\circ)\rangle$ with a fidelity of 0.986 ± 0.002 and show the reconstructed state in c) real part and d) imaginary part. In e) we show the measured coincidence counts for the state-discrimination measurement with feed-forward for the state from a) & b) (blue, left bars) and the state from c) & d) (red, right bars); from these counts we find that the probability for distinguishing these states is 0.9780 ± 0.0003, significantly exceeding the success probability for the best possible projective measurement without feed-forward, 0.922 ± 0.002.

of orthogonal two-qubit entangled states:

$$\begin{aligned} |\phi_0(\theta_0)\rangle &= \cos\theta_0|\mathbf{H}\rangle Z|u\rangle + \sin\theta_0|\mathbf{V}\rangle|u\rangle \\ |\phi_1(\theta_1)\rangle &= \cos\theta_1|\mathbf{H}\rangle Z|u^\perp\rangle - \sin\theta_1|\mathbf{V}\rangle|u^\perp\rangle, \end{aligned} \tag{1}$$

where $|\mathbf{H}\rangle$ ($|\mathbf{V}\rangle$) represent horizontal (vertical) polarization of a photon, $|u\rangle = \frac{\sqrt{3}}{2}|\mathbf{H}\rangle + \frac{1}{2}|\mathbf{V}\rangle$, $|u^\perp\rangle = \frac{1}{2}|\mathbf{H}\rangle - \frac{\sqrt{3}}{2}|\mathbf{V}\rangle$. While our parametrization does not allow the generation of arbitrary pairs of states, these pairs encapsulate the full difficulty of discrimination as optimal performance requires feed-forward for most values of θ_0 and θ_1. Note that any two orthogonal states can always be perfectly distinguished using local measurements *without* feed-forward when the states share no support in some product basis; this includes the cases where at least one of the states is a product state or maximally entangled.

We used HWPs S, A, and B to prepare the states in

Eq. 1 from our source. HWP S changes the Schmidt coefficients and HWPs A and B change the Schmidt basis; in principle, this setup can produce any pure 2-qubit entangled state with real coefficients. We vary θ_0 and θ_1 in steps of 15° from 0 to 90°, resulting in 49 pairs of states for which we can demonstrate state discrimination. We characterize each state by reconstructing its density matrix from a tomographically over-complete set of measurements $|\mathbf{H}\rangle$, $|\mathbf{V}\rangle$, $|\mathbf{D}\rangle = \frac{1}{\sqrt{2}}(|\mathbf{H}\rangle + |\mathbf{V}\rangle)$, $|\mathbf{A}\rangle = \frac{1}{\sqrt{2}}(|\mathbf{H}\rangle - |\mathbf{V}\rangle)$, $|\mathbf{R}\rangle = \frac{1}{\sqrt{2}}(|\mathbf{H}\rangle + i|\mathbf{V}\rangle)$, and $|\mathbf{L}\rangle = \frac{1}{\sqrt{2}}(|\mathbf{H}\rangle - i|\mathbf{V}\rangle)$ on each photon with the the Pockels cell off. The states were reconstructed using a semidefinite-program implementation [32] of the maximum-likelihood algorithm [33], and fidelities of the reconstructed density matrices with their targets range from 0.97 to 0.99.

The optimal state discrimination measurement is the same for all pairs of states of the form of Eq. 1. Alice measures in the basis $\{|\mathbf{H}\rangle, |\mathbf{V}\rangle\}$. If she registers outcome $|\mathbf{V}\rangle$, Bob will measure in the $\{|u\rangle, |u^{\perp}\rangle\}$ basis. On the other hand, if she measures $|\mathbf{H}\rangle$, the Pockels cell will fire on Bob's side, changing his measurement basis to $\{Z|u\rangle, Z|u^{\perp}\rangle\}$. We integrate coincidence counts for 100s, monitoring all four combinations of outputs ($\mathrm{T}_a\mathrm{T}_b$, $\mathrm{T}_a\mathrm{R}_b$, $\mathrm{R}_a\mathrm{T}_b$, $\mathrm{R}_a\mathrm{R}_b$). Here, T(R) refers to detection in the transmitted (reflected) arm of the PBS and the subscript a (b) labels Alice's (Bob's) analyzer.

Figs. 2a)-d) show the real and imaginary parts of the reconstructed density matrices for an example pair of states $|\phi_0(30°)\rangle$ and $|\phi_1(60°)\rangle$. They have fidelities 0.981 ± 0.002 and 0.986 ± 0.002 with the ideal states, respectively. Ideally, if we prepare any $|\phi_0(\theta_0)\rangle$ we should only detect counts in the $\mathrm{T}_a\mathrm{T}_b$ and $\mathrm{R}_a\mathrm{T}_b$ outputs, and if we prepare any $|\phi_1(\theta_1)\rangle$ we should only detect counts in $\mathrm{T}_a\mathrm{R}_b$ and $\mathrm{R}_a\mathrm{R}_b$. In Figs. 2e) we show the experimentally measured counts for the states in Figs. 2a) & b) (blue, left bars) and Figs. 2c) & d) (red, right bars). From these counts, we obtain the probability of correctly determining the state; for example, the probability of correctly determining $|\phi_0(\theta_0)\rangle$ is given by $P_0 = (n_{\mathrm{T}_a\mathrm{T}_b} + n_{\mathrm{R}_a\mathrm{T}_b})/\sum$, where $n_{\mathrm{T}_a\mathrm{T}_b}$ is the number of counts measured in the output $\mathrm{T}_a\mathrm{T}_b$, etc. and $\sum$ is the sum of all four coincidence counts when $|\phi_0(\theta_0)\rangle$ is prepared; a similar expression is used for the probability of correctly determining $|\phi_1(\theta_1)\rangle$, P_1. Using the counts measured for the target states $|\phi_0(30°)\rangle$ and $|\phi_1(60°)\rangle$ shown in Fig. 2e), we find the average probability for correctly determining the state is $P = 0.9780 \pm 0.0003$. The most significant difference from the theoretically perfect discrimination can be explained by our imperfect initial state fidelity.

For comparison, we consider a measurement strategy using local projective measurements *without* feed-forward, i.e., measurement in a basis $\{|\alpha\rangle, |\alpha^{\perp}\rangle\} \otimes \{|\beta\rangle, |\beta^{\perp}\rangle\}$, where $|\alpha\rangle$ and $|\beta\rangle$ are arbitrary single-photon polarization states. The optimal probability for distinguishing between pairs of states was found by numerically maximizing the success probability over all bases and all possible ways of assigning measurement results. We assume each state is produced with probability 0.5. Without feed-forward, the ideal states, $|\phi_0(30°)\rangle$ and $|\phi_1(60°)\rangle$, can be distinguished with only 0.933 probability and our experimental states, based on our tomography, can be distinguished with 0.922 ± 0.002 probability. Our experimental measurement $P = 0.9780 \pm 0.0003$ easily surpasses these limits, clearly demonstrating the advantage feed-forward provides in state discrimination.

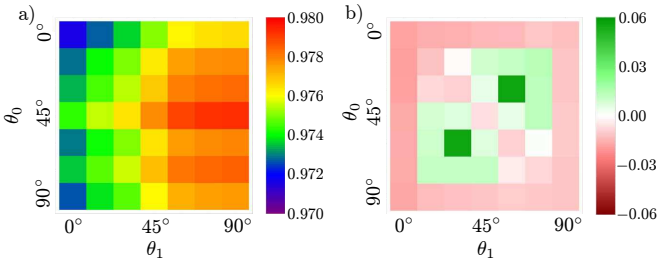

FIG. 3: Experimental minimum-error discrimination of orthogonal entangled states. a) Discrimination probability for pairs of states $|\phi_0(\theta_0)\rangle$ and $|\phi_1(\theta_1)\rangle$ for θ_0 and θ_1 ranging from 0° to 90° in steps of 15° using local measurements and feed-forward. All probabilities fall in the range from 0.9716 to 0.9793 with an average uncertainty (1 sd.) of 0.0003. In principle, these states can be discriminated perfectly by such a measurement, the difference being mostly attributable to our state preparation fidelity. b) The advantage between the measured discrimination probability and the optimal projective measurement *without* feed-forward on our experimentally produced states. The variation in the values show that some pairs of states are much easier to discriminate without feed-forward than others. We measure an advantage up to $5.6 \pm 0.2\%$.

In Fig. 3. In Fig. 3a) we show the measured discrimination probabilities for all pairs of states, which all fall in the range from 0.9716 to 0.9793. In Fig. 3b) we show the difference between our measured discrimination probability and the calculated optimal local measurement based on our tomographically reconstructed states. The maximum advantage our measurement achieved was $5.6 \pm 0.2\%$. Note that in several cases we have a slight disadvantage, up to $1.9 \pm 0.2\%$, as we are comparing our experimentally measured probability with feed-forward to the *best possible* theoretical measurement without.

In the second part of our experiment, we use our setup to perform minimum-error discrimination of equiprobable *non-orthogonal* entangled states of the form:

$$|\psi_0\rangle = \cos(45°-\eta)|\phi_0(60°)\rangle + \sin(45°-\eta)|\phi_1(30°)\rangle \quad (2)$$
$$|\psi_1\rangle = \sin(45°-\eta)|\phi_0(60°)\rangle + \cos(45°-\eta)|\phi_1(30°)\rangle.$$

Because these states have all real coefficients, we can prepare them using HWPs S, A, and B. The overlap between the states is $|\langle\psi_0|\psi_1\rangle|^2 = \cos^2 2\eta$. If $\eta = \pi/4$, the states are orthogonal, and if $\eta = 0$, the states are identical. Our

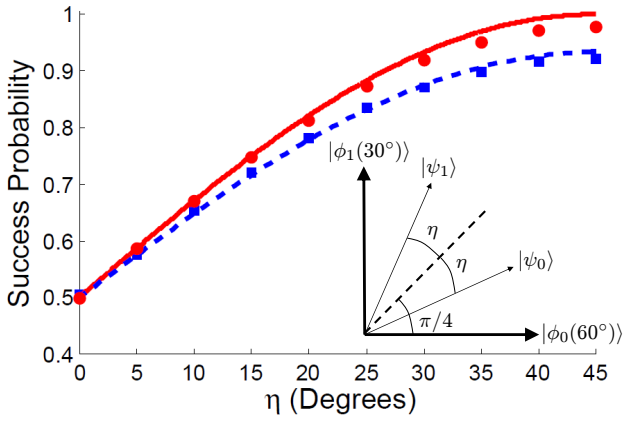

FIG. 4: Probabilities for successfully discriminating pairs of non-orthogonal states. In the inset, we depict non-orthogonal states $|\psi_0\rangle$ and $|\psi_1\rangle$ as superpositions of $|\phi_0(60°)\rangle$ and $|\phi_1(30°)\rangle$ with the angle η characterizing their overlap. The experimentally measured probabilities for distinguishing $|\psi_0\rangle$ and $|\psi_1\rangle$ (red circles), with errors, 0.0007, too small too see, and theoretical prediction given ideal state preparation (red solid line) are shown as a function of η. The data follow the prediction closely, taking the initial fidelity into account. The best possible discrimination probability by local projective measurements without feed-forward is shown for the ideal states (blue dashed line) and from the tomographically reconstructed states (blue squares). Our results show a distinct advantage arising from feed-forward.

measurement can, in principle, perfectly distinguish the states $|\phi_0(60°)\rangle$ and $|\phi_1(30°)\rangle$ which corresponds to the minimum-error, or Helstrom measurement for these pairs of states when they are prepared with equal probability.

Fig. 4 shows the experimentally measured probability for distinguishing pairs of non-orthogonal states (red circles) as a function of the overlap parameter η. We observe good agreement between the data and theoretical expectation (red solid line). The ratio of the experimental results to the theoretical expectations ranges from $99.9 \pm 0.2\%$ for nearly identical states (η=0) to $97.65 \pm 0.03\%$ for nearly orthogonal states (η=45°); again, this difference is mostly due to experimental state preparation fidelity. The probabilities for the best possible discrimination using local projective measurements without feed-forward are shown in Fig. 4 for the experimentally produced states (blue squares) reconstructed via tomography and for the ideal states (blue dashed line). Our experimental state discrimination results show a clear advantage over both of these quantities.

Optimal quantum state discrimination plays an important role in quantum information. We have implemented optimal minimum-error discrimination of orthogonal and non-orthogonal entangled quantum states using only local measurements and feed-forward. Our experimental results show a clear advantage over the best possible projective measurement without feedforward. This demonstrates a rather surprising ability of local measurements to distinguish global properties, i.e., entanglement, and is the first implementation of a state discrimination protocol in a uniquely quantum regime.

The authors gratefully acknowledge financial support from NSERC, QuantumWorks, MRI ERA, the Perimeter Institute and CFI. Research at the Perimeter Institute is supported by Industry Canada and by the Ontario MRI.

* Electronic address: kresch@iqc.ca

[1] A. Chefles, Contemporary Phys. **41**, 401 (2000).
[2] S.M. Barnett and S. Croke, Adv. Opt. Phot. **1**, 238 (2009).
[3] C.W. Helstrom, Quantum Detection and Estimation Theory (Academic, 1976).
[4] A.S. Holevo, J. Multivariate Analysis **3**, 337 (1973).
[5] H.P. Yuen, R.S. Kennedy, and M. Lax, IEEE Trans. Inf. Theory **IT-21**, 125 (1975).
[6] I.D. Ivanovic, Phys. Lett. A **123**, 257 (1987).
[7] D. Dieks, Phys. Lett. A **126**, 303 (1988).
[8] A. Peres, Phys. Lett. A **128**, 19 (1988).
[9] E.B. Davies, IEEE Trans. Inf. Theory **IT-21**, 596 (1978).
[10] M. Sasaki *et al.*, Phys. Rev. A **59**, 3325 (1999).
[11] S. Croke *et al.*, Phys. Rev. Lett **96**, 070401 (2006).
[12] S.M. Barnett and E. Riis, J. Mod. Opt. **44**, 1061 (1997).
[13] R.M.B. Clarke *et al.*, Phys. Rev. A **64**, 012303 (2001).
[14] B. Huttner *et al.*, Phys. Rev. A **54**, 3783 (1996).
[15] R.B.M. Clarke *et al.*, Phys. Rev. A **63**, 040305 (2001).
[16] M. Mohseni *et al.*, Phys. Rev. Lett. **93**, 200403 (2004).
[17] J. Mizuno *et al.*, Phys. Rev. A **65**, 012315 (2001).
[18] P.J. Mosley *et al.*, Phys. Rev. Lett. **97**, 193601 (2006).
[19] B.L. Higgins *et al.*, Phys. Rev. Lett. **103**, 220503 (2009).
[20] J. Calsamiglia, and N. Lütkenhaus, Appl. Phys. B **72**, 67 (2001).
[21] C.H. Bennett *et al.*, Phys. Rev. A **59**, 1070 (1999).
[22] J. Walgate *et al.*, Phys. Rev. Lett. **85**, 4972 (2000).
[23] S. Virmani et al., Phys. Lett. A **288**, 62 (2001).
[24] Y.-X. Chen and D. Yang, Phys. Rev. A **64**, 064303 (2001).
[25] Y.-X. Chen and D. Yang, Phys. Rev. A **65**, 022320 (2002).
[26] Z. Ji *et al.*, Phys. Rev. A **71**, 032323 (2005).
[27] T. Kim *et al.*, Phys. Rev. A **73**, 012316 (2006).
[28] A. Fedrizzi et al., Optics Express **15**, 15377 (2007).
[29] D.N. Biggerstaff et al., Phys. Rev. Lett. **103**, 240509 (2009).
[30] R. Jozsa, J. Mod. Opt. **41**, 2315 (1994).
[31] The tangle is the square of the concurrence. V. Coffman *et al.*, Phys. Rev. A **61**, 052306 (2000).
[32] A.C. Doherty *et al.*, unpublished (2009).
[33] D.F.V. James *et al.*, Phys. Rev. A **64**, 052312 (2001).